Plant, Cell & Environment

Plant, Cell and Environment (2015) doi: 10.1111/pce.12538

Original Article

Proteomic analysis provides new insights into the adaptive response of a dinoflagellate *Prorocentrum donghaiense* to changing ambient nitrogen

Ying-Jiao Zhang[1,2], Shu-Fei Zhang[1], Zhi-Ping He[1], Lin Lin[1] & Da-Zhi Wang[1]

[1]*State Key Laboratory of Marine Environmental Science, College of the Environment and Ecology, Xiamen University, Xiamen 361102, China and* [2]*Institute of Urban Environment, Chinese Academy of Sciences, Xiamen 361021, China*

ABSTRACT

Nitrogen (N) is the major nutrient limiting phytoplankton growth and productivity over large ocean areas. Dinoflagellates are important primary producers and major causative agents of harmful algal blooms in the ocean. However, very little is known about their adaptive response to changing ambient N. Here, we compared the protein profiles of a marine dinoflagellate *Prorocentrum donghaiense* grown in inorganic N-replete, N-deplete and N-resupplied conditions using 2-D fluorescence differential gel electrophoresis. The results showed that cell density, chlorophyll *a* and particulate organic N contents presented low levels in N-deplete cells, while particulate organic carbon content and glutamine synthetase (GS) activity maintained high levels. Comparison of the protein profiles of N-replete, N-deplete and N-resupplied cells indicated that proteins involved in photosynthesis, carbon fixation, protein and lipid synthesis were down-regulated, while proteins participating in N reallocation and transport activity were up-regulated in N-deplete cells. High expressions of GS and 60 kDa chaperonin as well as high GS activity in N-deplete cells indicated their central role in N stress adaptation. Overall, in contrast with other photosynthetic eukaryotic algae, *P. donghaiense* possessed a specific ability to regulate intracellular carbon and N metabolism in response to extreme ambient N deficiency.

Key-words: 2-D fluorescence differential gel electrophoresis ; nitrogen; glutamine synthetase.

INTRODUCTION

Nitrogen (N) is an essential macronutrient for marine phytoplankton as it is the major component of proteins, nucleic acids, chlorophyll and other macromolecules (Hockin *et al*. 2012). N limitation occurs in large segments of the world's oceanic, coastal and estuarine waters, and constrains primary productivity (Howarth 1988; Gruber 2004). N deficiency inhibits cell growth, changes pigment composition, decreases photosynthetic energy harvesting and reduces the efficiency of photosynthesis (Kolber *et al*. 1988; Herzig & Falkowski 1989; Geider *et al*. 1993, 1998; Latasa & Berdalet 1994). Moreover, N limitation increases phytoplankton susceptibility to ultraviolet and their ability to counteract photodamage (Litchman *et al*. 2002). Therefore, the capacity of phytoplankton to respond to changing ambient N is essential to their success in the ocean (Fawcett & Ward 2011).

Dinoflagellates are important primary producers and major causative agents of harmful algal blooms (HABs) in the ocean (Hackett *et al*. 2004). Moreover, dinoflagellate species produce potent toxins that can cause shellfish poisoning and adverse impacts on the environment, the economy and human health (Van Dolah 2000). Dinoflagellate HABs have attracted considerable attention around the world. Much effort has been devoted to the physical, chemical and ecological properties during the course of *in situ* dinoflagellate blooms in order to understand the mechanisms controlling the occurrence and maintenance of these blooms at the population level (McGillicuddy *et al*. 2005). The growing evidence suggests that the eutrophication caused by the anthropogenic inputs of N to the coastal area is one of the major reasons resulting in the occurrence of HABs (Heisler *et al*. 2008). Therefore, understanding the cellular responses of the dinoflagellates to the absence or presence of N is important to any understanding of the formation mechanism of blooms (Dagenais-Bellefeuille & Morse 2013).

Studies show that N availability affects cell growth, cellular N and chlorophyll *a* (Chl *a*) content as well as toxin production of dinoflagellates (Boyer *et al*. 1987; Anderson *et al*. 1990; Flynn *et al*. 1994; McLachlan *et al*. 1994; Wang & Hsieh 2002; Li *et al*. 2011a). Lack of N is regarded as the main trigger for encystment in some dinoflagellates (Chapman & Pfester 2008). The alteration of protein expression profiles caused by changing ambient N has also been observed in several dinoflagellate species (Chan *et al*. 2004; Wang *et al*. 2012). Two plastid proteins, ribulose-1,5-bisphosphate carboxylase oxygenase form II and N-associated protein 50, are down-regulated in N-depleted *Alexandrium affine* (Lee *et al*. 2009). The high expressions of nitrate transport, signal transduction, amino acid metabolism, DNA repair and hemolysin manufacture are also observed in N-deprived *Karenia mikimotoi* (Lei & Lü 2011). Thus, a better understanding of proteomic responses to N-depletion and

Correspondence: D.-Z. Wang. e-mail: dzwang@xmu.edu.cn

N-resupplement may contribute both to our understanding of the adaptive mechanism of dinoflagellates to changing ambient N and to revealing the formation mechanism of dinoflagellate blooms.

P. donghaiense is a key dinoflagellate species that causes extensive blooms along the coast of China, and results in serious damage to the ecosystem and mariculture (Zhou *et al*. 2003). Much effort has been devoted to *in situ* investigations of environmental conditions regulating the occurrence and maintenance of *P. donghaiense* blooms, and N-induced coastal eutrophication has been shown to play an important role in the initiation and maintenance of *P. donghaiense* blooms (Zhou *et al*. 2003; Zhou 2010). *P. donghaiense* can utilize a wide range of N substrates, including NO_3^-, NH_4^+, and urea (Li *et al*. 2011b), and can survive long periods in N-deplete condition (Lu 2004), indicating that it might possess a specific adaptive response mechanism to ambient N stress. However, very little is known about it. Our study investigated the physiological and proteomic responses of *P. donghaiense* to N-depletion, compared the protein profiles of *P. donghaiense* under N-replete, N-deplete and N-resupplied conditions using a quantitative proteomic approach, two-dimensional fluorescence differential gel electrophoresis (2-D DIGE), and characterized the differentially expressed proteins using matrix-assisted laser desorption/ionization time-of-flight/time-of-flight (MALDI-TOF-TOF) mass spectrometry (MS). The purpose of this study was to identify the proteins responding to ambient N variation and gain insight into the global regulation of metabolic pathways in response to N-depletion and N-resupplement.

MATERIALS AND METHODS

Organism and culture conditions

The strain of *P. donghaiense* was provided by the Culture Collection Center of Marine Algae of the State Key Laboratory of Marine Environmental Science, Xiamen University, China. Batch cultures of axenic *P. donghaiense* were maintained in 5 L bottles in K medium (Keller *et al*. 1987) using 0.22 μm filtered, autoclaved natural seawater (30 psu) at 19 °C under a 14 h:10 h light : dark photoperiod at a light intensity of approximately 100 μmol photons m^{-2} s^{-1} provided by fluorescent lamps.

The experimental design included three groups, N-replete, N-deplete and N-resupplied. *P. donghaiense* cells in the early exponential growth phase were harvested using centrifugation (5000 g for 10 min at 19 °C), washed twice with sterile seawater, and inoculated into nine bottles each with 10 L of sterile seawater with undetectable N to yield an initial cell density of 4000 cell mL^{-1}. K medium without N source was used for N-deplete culture. In N-replete culture, 50 μM ammonium and 882 μM nitrate were added to the culture media at the beginning of the experiment. In N-resupplied experiment, 50 μM ammonium and 882 μM nitrate were added to the N-deplete culture at day 7. Each group had triplicate biological repeats.

Physiological parameter analysis

Cell density was monitored at the same time each day from a 1 mL aliquot removed from each bottle and fixed with 10 μL of Lugol's solution. Cells were counted under a light microscope using a Sedgwick Rafter cell counter. Cell growth rate was calculated based on the following formula where N_t was the number of cells per mL at time t, N_0 the number at time 0, and t was the duration between times t and 0 (Costas 1990).

$$\text{div } d^{-1} = \frac{1}{\ln(2)} \cdot \frac{\ln\left(\frac{N_t}{N_0}\right)}{t}$$

Chl *a* samples (50 mL from each bottle) were filtered through 25 mm glass fiber filters (Whatman type GF/F), extracted using 90% acetone and determined using *in vitro* fluorometric methods (Xu *et al*. 2012). Algal cells (2 mL from each bottle) were dark-adapted for 15 min before measuring the maximum photochemical efficiency of PSII in the dark-adapted state (*Fv/Fm*) using a PHYTO-PAM (Walz GmbH, Effeltrich, Germany). Samples for particulate organic carbon (POC) and particulate organic nitrogen (PON) (100 mL from each bottle) were filtered through a 25 mm pre-combusted (450 °C, 4 h) GF/F filter. The cells on the filters were exposed to HCl fumes and oven-dried at 65 °C for 24 h to remove inorganic carbon and nitrogen before analysis. POC and PON were determined using a PE 2400 Series II CHNS elemental analyzer (Perkin Elmer, Norwalk, CT, USA) following JGOFS protocols (Knap *et al*. 1996).

Glutamine synthetase (GS) activity analysis

Samples (200 mL from each bottle) were filtered through nucleopore membranes (3 μm) and washed twice with sterile seawater. Proteins were extracted following a previously reported protocol (Wang *et al*. 2009). Briefly, cells were added to 1 mL extraction buffer containing 50 mmol L^{-1} Tris-HCl (pH 7.5), 2 mmol L^{-1}dithiothreitol (DTT), 2.5 mmol L^{-1} $MgCl_2$, and 1 mmol L^{-1}ethylenediaminetetraacetic acid and disrupted with 0.5 mm glass beads in a mini-beadbeater (Biospec Products, Bartlesville, OK, USA) at 2500 r.p.m. for seven bursts of 20 s with 1 min ice cooling in each burst-interval. The solution was centrifuged at 10 000 *g* for 35 min at 4 °C, subsequently 0.1 mL 100 mmol L^{-1}streptomycin sulphate was added to the supernatant to remove nucleic acids. After reaction for 15 min at 4 °C, the supernatant was centrifuged at 8000 *g* for 30 min at 4 °C and the resulting supernatant was then tested for GS activity.

GS activity was estimated following Wang *et al*. (2009) by determining the amount of inorganic phosphate. Briefly, 100 μL enzyme crude extract was added to the reaction buffer containing 123 μL 1 mol L^{-1} imidazole hydrochloride buffer, pH7.8, 100 μL 10 mmol L^{-1} NH_4Cl, 20 μL 60 mmol L^{-1} ATP, pH7.8, 17 μL 1.67 mol L^{-1} $MgCl_2$, and 100 μL 1 mol L^{-1} sodium glutamate, pH 7.8, and stored at 25 °C for 30 min. The reaction was initiated immediately after enzyme extract addition and stopped by adding 1.8 mL $FeSO_4 \cdot 7H_2O$ (0.8% w/v in

7.5 mmol L^{-1} H_2SO_4). Meanwhile, a time-zero control and a reagent blank were set up to eliminate interference from inorganic phosphate of phosphatases and ATPases in the crude extract. The time-zero control contained all components of the reaction system, but was stopped at initiation, and the reagent blank was incubated for 30 min at 25 °C without enzyme crude extract. Thereafter, 0.15 mL of colour-forming reagent ammonium molybdate (6.6% w/v in 3.75 mol L^{-1} H_2SO_4) was added and vortexed vigorously. After 15 min of chromogenic reaction, the amount of inorganic phosphate was measured using a spectrophotometer. The enzyme activity was presented by the amount of inorganic phosphate liberated per cell per minute (fmol $cell^{-1}$ min^{-1}).

Protein extraction

To compare differential protein expression, *P. donghaiense* cells were harvested from four conditions: the N-replete cells were harvested at the exponential growth phase (day 3); the N-deplete cells were harvested at day 7; and after addition of N for 2 and 26 h, the cells were harvested as N-resupplied-2h and N-resupplied-26h. For each sample, approximately 1×10^7 *P. donghaiense* cells were collected at hour 4 of the 14 h light cycle using centrifugation at 8000 *g* for 10 min at 20 °C. Each pellet was subsequently transferred to a 1.5 mL microcentrifuge tube and resuspended with 1 mL TRIzol reagent (Invitrogen, Carlsbad, CA, USA). Total proteins were extracted following a previously reported protocol (Wang *et al*. 2013). Briefly, cells were disrupted with sonication; protein was extracted using TRIzol, chloroform and ethanol and precipitated using isopropanol. The protein obtained was briefly washed with 95% ethanol before being allowed to air dry. Then 100 μL of rehydration buffer containing 7 M urea (Bio-Rad, Hercules, CA, USA), 2 M thiourea (Sigma, St Louis, MO, USA), 2% CHAPS (Bio-Rad), 1% DTT (Bio-Rad), 0.5% immobilized pH gradient (IPG) buffer (GE Healthcare, San Francisco, CA, USA), and a trace of bromophenol blue (Bio-Rad) were added to solubilize the protein pellet. The solution was centrifuged at 20 000 *g* for 30 min at 16 °C and the supernatant was collected for 2-D DIGE analysis. The protein content was quantified using a 2-D Quant kit (GE Healthcare), and Student's *t*-test was used to determine the significance ($P < 0.05$ or $P < 0.01$) of the cellular protein content.

2-D DIGE and image analysis

Protein labelling was carried out following the manufacturer's protocol and instructions (GE Healthcare). Each group (N-replete, N-deplete and N-resupplied) contained triplicate biological repeats, generating 12 individual samples that were co-resolved across six DIGE gels all coordinated using the same pooled sample internal standard to reduce inter-gel variation. Experiments utilizing 24 cm pH 4–7 isoelectric focusing (IEF) gradients containing 120 μg of total protein were equally divided between any two samples and an aliquot of the internal standard as follows: proteins in each sample were fluorescently tagged with a set of matched fluorescent dyes based on the standard protocol for minimal labelling. To eliminate any dye-specific labelling artefacts, three samples of each group were labelled with Cy3, Cy5 or a mixture of these two, the paired sample being mixed with a Cy2-labelled pooled standard. In every case, 320 pmol of dye was used for 40 μg of protein. Labelling was performed for 30 min on ice in darkness and the reactions were stopped with the addition of 1 μL of 10 mM L-lysine for 10 min on ice under the same conditions.

The mixtures containing 120 μg of protein were brought up to a final volume of 450 μL with 1 × rehydration buffer, after which 0.5% IPG buffer was added and they were mixed thoroughly. The labelled samples were then applied to the strips on an Ettan IPGphor III Isoelectric Focusing System (GE Healthcare) at 62 kV h^{-1} in different phases as follows: 6 h at 40 V, 6 h at 100 V, 30 min ramp up to 500 V, 1 h ramp up to 1000 V, 1 h ramp up to 2000 V, 1.5 h ramp up to 10 000 V, and 60 kV h^{-1} at 10 000 V.

After the first dimension was run, each strip was equilibrated with about 10 mL equilibration buffer containing 50 mM Tris (pH 8.8), 6 M urea, 30% glycerol, 2% sodium dodecyl sulphate (SDS), 1% DTT and a trace amount of bromophenol blue for 16 min. The strip was then placed in fresh equilibration buffer containing 2.5% iodoacetamide (instead of DTT) for another 16 min. Second dimension SDS-polyacylamide gel electrophoresis was run by overlaying the strips on 12% isocratic Laemmli gels (24 × 20 cm), which were cast in low fluorescence glass plates, on an Ettan DALT VI system (GE Healthcare). Gels were run at 10 °C at a constant power of 1 W gel^{-1} during 30 min followed by 15 W gel^{-1} until the bromophenol blue tracking front had run off the gel. Fluorescent images of the gels were acquired on a Typhoon 9400 scanner (GE Healthcare). Cy2, Cy3 and Cy5 images for each gel were scanned at 488/520, 532/580 and 633/670 nm excitation/emission wavelengths, respectively, at 100 μm resolution, thus a total of 18 images were obtained from the six gels (6 × 3, Table 1).

Image analysis was performed using DeCyder version 6.0 software (GE Healthcare) following the manufacturer's recommendations. The differential in-gel analysis (DIA) module

Table 1. Two-dimensional fluorescence differential gel electrophoresis experimental design

Number of gel	Cy2	Cy3	Cy5
1	Internal standard	N-replete (1)	N-resupplied-26h (1)
2	Internal standard	N-resupplied-2h (1)	N-deplete (1)
3	Internal standard	N-replete (2)-deplete (2)	N-resupplied-26h (2)
5	Internal standard	N-deplete (3)	N-replete (3)
6	Internal standard	N-resupplied-26h (3)	N-resupplied-2h (3)

was used for processing images from a single gel. The number of initial spot detection was 1500. The biological variation analysis module was used for inter-gel matching of internal standard and samples across all gels and performing comparative cross-gel statistical analyses of all spots based on spot volumes. Only spots present in 15 or more gel images were considered and proteins whose abundance presented a relative change of twofold (Student's *t*-test, $P < 0.05$) or greater, permitting the detection of differentially expressed spots between experimental conditions (Barcelo-Batllori *et al*. 2008). Finally, matches and the data quality of proteins of interest were manually checked to avoid false positives. Relative changes of protein abundances from N-deplete versus N-replete, N-resupplied-2h versus N-replete, N-resupplied-26h versus N-replete, and N-replete versus N-replete, were applied to create the heat map using the heatmap.2 method in package gplots of R Project.

Protein identification

Preparative 2-D gels had a higher protein load (350 μg) for the four samples and were silver stained using the previously described method (Wang *et al*. 2010). Owing to the selective staining properties of CyDye labelling and silver staining, 56 spots were visible and were excised from the silver-stained gels. Each set of spots was excised from replicate gels, destained and in-gel digested with trypsin (Promega, Southampton, UK) at 37 °C overnight.

Samples were analysed using an AB SCIEX MALDI TOF-TOF™ 5800 Analyzer (Applied Biosystems, Foster City, CA, USA) equipped with a neodymium: yttrium-aluminum-garnet laser (laser wavelength was 355 nm), using reflection positive ion mode. Protein identification was conducted following the multi-layered identification method previously described (Wang *et al*. 2011). Briefly, the MS and MS/MS spectra of each protein spot obtained from MALDI-TOF-TOF MS were first submitted to a MASCOT search against the NCBI database with no taxonomic restriction. If the database entries were matched with at least two peptides and the protein scores taken from the MS combined MS/MS search had a minimum confidence interval (CI) of 95%, the protein hits were regarded as confident identifications. Once a protein's CI was below 95%, the MS/MS spectra of each protein spot was searched against the dinoflagellate expressed sequence tag database, and it was considered to be significant with the total ion CI % ≥ 95, and the *E*-value < e^{-20}. Those remaining non-confident hits were further subjected to *de novo* interpretation using DeNovo Explorer software (Applied Biosystems). The *de novo* sequences passing a reliability filter were subsequently submitted to non-redundant MS-BLAST searches. Only high-scoring segment pairs with a score of 62 or above were considered to be confident.

Immunoblot analysis

To further validate the 2-D DIGE results, ribulose 1,5-bisphosphate carboxylase oxygenase (RuBisCo) form II was selected for Western blot analysis based on its higher-fold difference on DIGE analysis. For each sample, 20 μg protein was incubated at 95 °C for 5 min and separated on 12.0% SDS-polyacrylamide gels (Hoefer SE 600 Ruby, GE Healthcare) using the Laemmli buffer system. The proteins were transferred to a polyvinylidene difluoride membrane (Millipore, Bedford, UK) using a Trans-Blot SD Semi-Dry Transfer Cell (Bio-Rad) at 200 mA for 3 h. The membrane was blocked with 5% non-fat dry milk for 2 h and then incubated for 2 h at room temperature with the primary antibody at 1:1000 dilution: a dinoflagellate anti-RuBisCo form II (an antiserum raised against the *Prorocentrum minimum* form II RuBisCo, Zhang & Lin 2003) and anti-tubulin (Beyotime, Shanghai, China). Following three washes in phosphate-buffered saline containing 0.05% Tween 20 (PBST), the membrane was incubated with a secondary anti-rabbit IgG (1:1000 dilution; Beyotime) for 1 h at room temperature and then washed five times in PBST. Finally, the immunoblotting image was visualized using the Enhanced Chemiluminescent Substrate (Invitrogen) and the intensity of the bands was determined using densitometric analysis. The target protein signals were normalized to the tubulin signal and analysed semiquantitatively using a Quantity One (Bio-Rad) system. It should be pointed out that there are few dinoflagellate antibodies available for protein validation at present. Student's *t*-test was used to determine the level of significance ($P < 0.05$ or $P < 0.01$).

RESULTS

Physiological responses of *P. donghaiense* to N nutrient variations

Physiological responses of *P. donghaiense* to N depletion and resupplement are shown in Figs 1 and 2. Starting from a cell density of approximately 4000 cells mL^{-1}, the N-replete culture of *P. donghaiense* exhibited a low growth rate of 0.19 at day 1, then grew rapidly with an average growth rate of 0.73 per day from days 2 to 7, and entered the stationary phase from days 8 to 10 with an average growth rate of 0.01 per day. In the N-deplete culture, the cell growth rate was 0.08 and 0.64 at days 1 and 2, respectively. Then a low average growth rate of 0.05 per day from days 3 to 10 was maintained. In the N-resupplied culture, cells recovered rapidly with a high growth rate of 0.58 per day from days 8 to 10 (Fig. 1a).

The cellular Chl *a* content of the N-replete culture increased a little, from 2.2 μg Chl *a* per cell at day 0 to 3.4 μg Chl *a* per cell at day 2, but then decreased gradually to a low level (Fig. 1b). For the N-deplete culture, the cellular Chl *a* content decreased continuously, from 1.9 μg Chl *a* per cell at day 0 to 0.8 μg Chl *a* per cell at day 10. However, the cellular Chl *a* content of N-deplete cells increased rapidly following N resupplement at day 7.

The photochemical efficiency of PSII (*Fv/Fm*) increased significantly in the first 2 d (up to 0.6) and then decreased slowly throughout the experiment in N-replete cells. For the N-deplete culture, *Fv/Fm* maintained a relatively stable low level. However, it increased rapidly and reached a high level (about 0.6) after resupplying N for 3 d (Fig. 1c).

The PON content increased from 32 pg N per cell at day 0 to 58 pg N per cell at day 2, then decreased gradually to

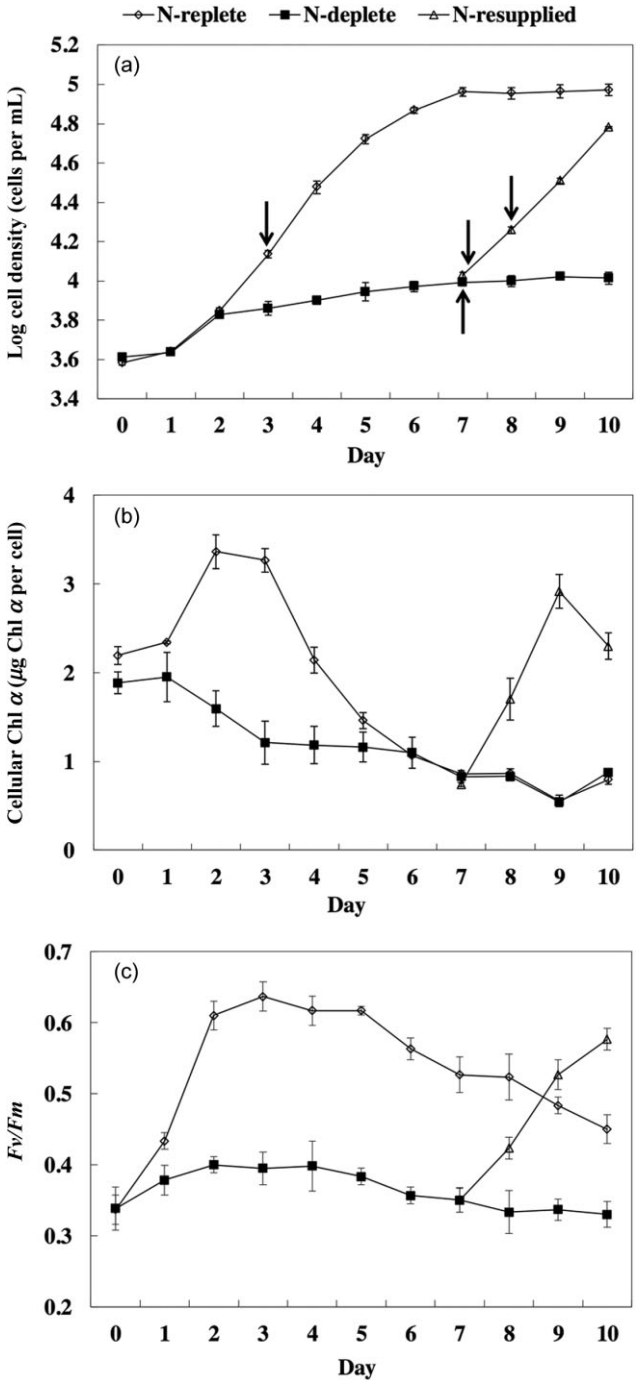

Figure 1. Variations of cell density, chlorophyll *a* content and *Fv/Fm* of *Prorocentrum donghaiense* grown in N-replete, N-deplete and N-resupplied conditions. After the cells were starved for 7 d, 50 μM ammonium and 882 μM nitrate were added to the N-deplete culture medium. (a) Cell density; (b) chlorophyll *a*; (c) *Fv/Fm*. Results are shown as means of three biological replicates ± standard deviation. The arrows represent the sampling time.

27 pg N per cell at day 10 in N-replete cells (Fig. 2a). However, it maintained a relatively stable level in N-deplete cells, around 35 pg N per cell. After resupplying N at day 7, it sharply increased from 37 pg N per cell at day 7 to 72 pg N per cell at day 8, and then decreased to 40 pg N per cell at day 10 (Fig. 2a). The POC content reached a high level at day 2 in both N-replete and N-deplete cultures, about 317 pg C per cell and 353 pg C per cell, respectively. Then, it decreased

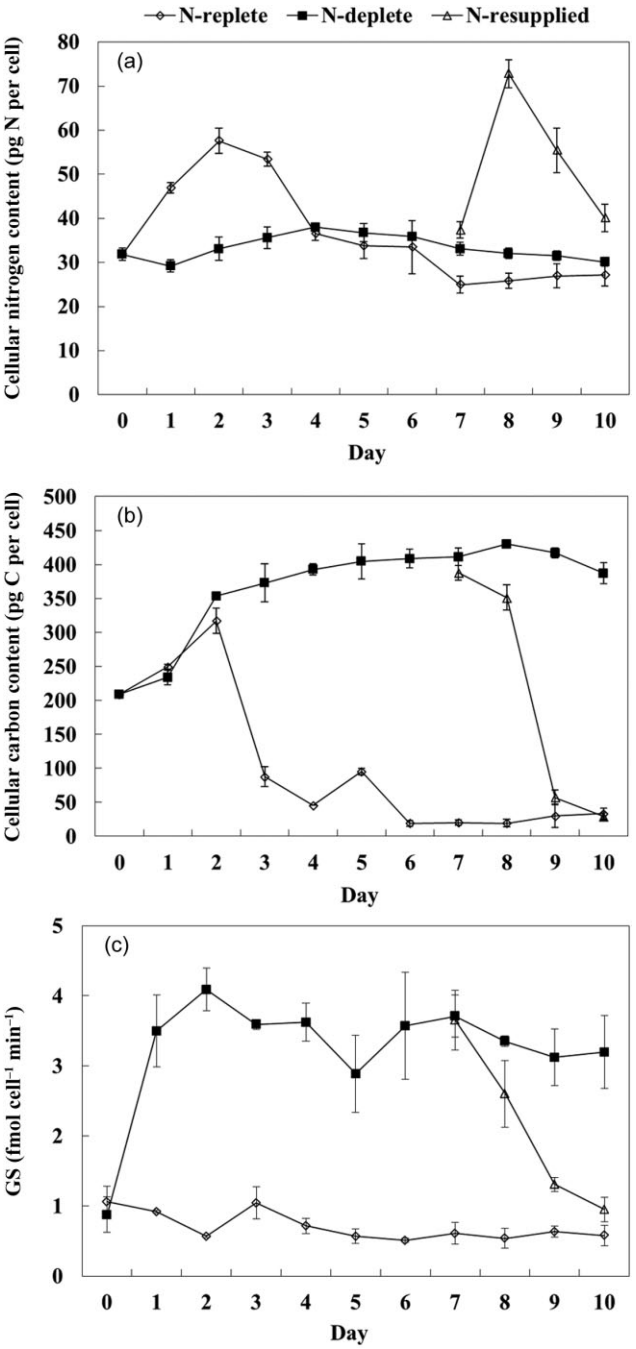

Figure 2. Variations of particulate organic carbon and nitrogen contents and glutamine synthetase (GS) activity of *Prorocentrum donghaiense* grown in N-replete, N-deplete and N-resupplied conditions. After the cells were starved for 7 d, 50 μM ammonium and 882 μM nitrate were added to the N-deplete culture medium. (a) Particulate organic nitrogen; (b) particulate organic carbon; (c) GS activity. Results are shown as means of three biological replicates ± standard deviation. Different lowercase letters indicate statistically significant difference at $P < 0.05$.

rapidly in N-replete cells and reached a low level, while it maintained a high and stable level in N-deplete cells. After resupplying N to N-deplete cells at day 7, it sharply decreased from 387 pg C per cell at day 7 to 29 pg C per cell^{-1} at day 10 (Fig. 2b).

Variations of GS activity of *P. donghaiense* under various N conditions

The GS activity of N-replete cells remained at a low level throughout the experiment, about 1 fmol cell^{-1} min^{-1} (Fig. 2c). However, it increased rapidly in N-deplete cells in the first 2 d, from 1 fmol cell^{-1} min^{-1} at day 0 to 4 fmol cell^{-1} min^{-1} at day 2, and then it maintained a relatively constant high level. After resupplying N to the N-deplete cells at day 7, it sharply decreased to a low level (about 1 fmol cell^{-1} min^{-1}) within 3 d. These results suggested that GS might play an important role in N stress adaptation in *P. donghaiense*.

2-D DIGE analysis of differentially expressed proteins

The 2-D DIGE proteomic approach was applied to analyse the protein alterations in N-replete, N-deplete and N-resupplied cells. To monitor protein expression, four samples, N-replete, N-deplete and N-resupplied-2h and N-resupplied-26h were selected. Based on the DIA module analysis, 1250 ± 90, 1251 ± 85, 1260 ± 98 and 1310 ± 4 protein spots were detected in N-replete, N-deplete, N-resupplied-2h and N-resupplied-26h cells. Among them, 56 protein spots presented statistically significant alterations in abundance (analysis of variance-1, $P \leq 0.05$), all greater than twofold (Fig. 3a). For the altered protein spots, 48 were detected localized in N-deplete versus N-replete images (22 up-regulated and 26 down-regulated proteins), 53 were detected localized in N-resupplied-2h versus N-replete images (21 up-regulated and 32 down-regulated proteins), two were detected localized in N-resupplied-26h versus N-replete images (both up-regulated). Based on the heat map analysis (Fig. 3b), the protein spots between N-replete and N-resupplied-26h, and the protein spots between N-deplete and N-resupplied-2h presented similar expression patterns, indicating the rapid proteomic response of *P. donghaiense* to ambient N changes.

Protein identification and variation of the N-responsive proteins

All the altered protein spots were submitted for identification using MALDI-TOF-TOF MS and 37 protein spots were identified. However, 19 protein spots did not obtain positive identification and had to be assigned as unknown. It was noted that a few protein spots were identified as the same protein with different MW and/or p*I* values. These proteins might represent different modifications of the same gene product or isoforms of the same protein family. NCBI ID number, protein name, and average relative change at each time point for the proteins identified are listed in Table 2. Detailed information including NCBI ID number, protein name, theoretical p*I* value and molecular weight, protein score, as well as the protein score CI % for the proteins identified are listed in Supporting Information Tables S1–S4.

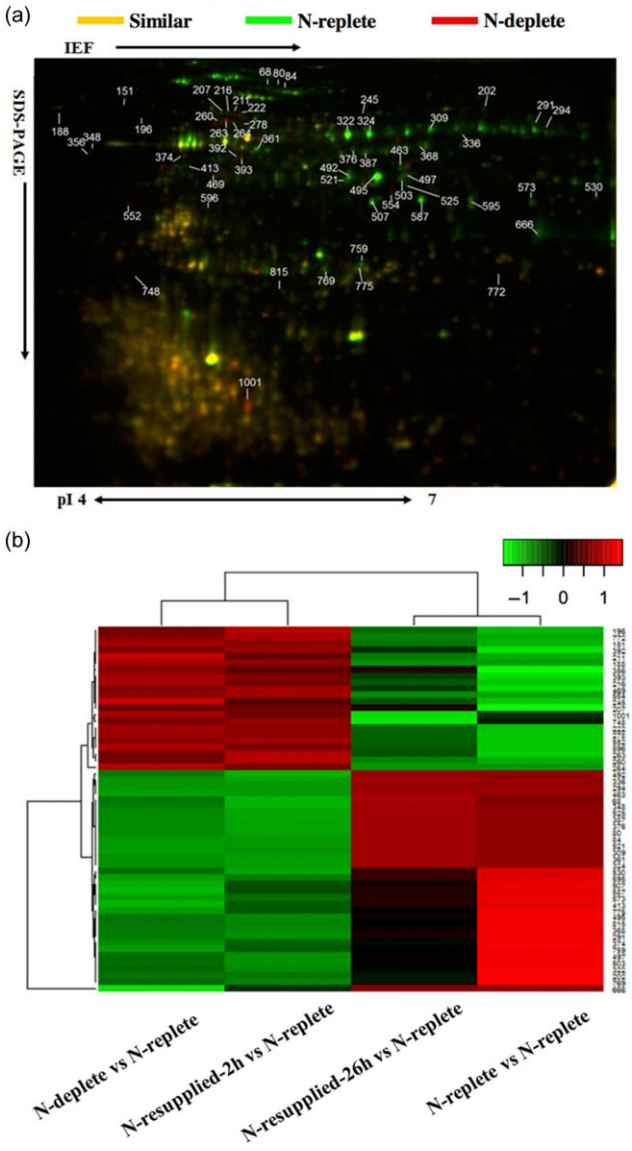

Figure 3. Two-dimensional fluorescence differential gel electrophoresis (2-D DIGE) analysis of *Prorocentrum donghaiense* in N-replete, N-deplete, N-resupplied-2h and N-resupplied-26h conditions. (a) The representative gel shows the total 56 protein spots with statistically significant alterations (cy3: N-deplete, cy5: N-replete). Yellow spots represent similar protein abundance, red spots represent proteins more abundant in N-deplete cultures, while green spots represent proteins more abundant in N-replete. (b) The heat map of the 56 differentially expressed protein spots. Fold change values are shown for the N-deplete versus N-replete, N-resupplied-2h versus N-replete, N-resupplied-26h versus N-replete and N-replete versus N-replete, with up-regulation denoted in red and down-regulation denoted in green.

Table 2. Differentially expressed proteins of *Prorocentrum donghaiense* cells in different N conditions

			N-deplete versus N-replete		N-resupplied-2h versus N-replete		N-resupplied-26h versus N-replete		
Spot ID[a]	Protein name	NCBI[b]	Ratio[c]	*P* value	Ratio[c]	*P* value	Ratio[c]	*P* value	1-ANOVA
Nitrogen metabolism									
260	Glutamine synthetase	1707964	4.6	0.033	5.4	0.0068	1.5	0.15	0.0051
263	Glutamine synthetase	1707964	4.3	0.034	5.0	0.007	2.3	0.27	0.023
264	Glutamine synthetase	1707964	8.4	0.011	7.2	0.052	1.0	0.98	0.0095
278	Glutamine synthetase	154629	3.8	0.015	3.7	0.015	1.8	0.37	0.019
Stress response									
207	60 kDa chaperonin 1	118597092	2.0	0.022	2.0	0.027	1.8	0.049	0.034
211	60 kDa chaperonin	14916973	3.2	0.0073	2.6	0.021	1.3	0.42	0.0063
245	60 kDa chaperonin	33152794	2.0	0.01	1.7	0.031	1.3	0.39	0.045
80	Heat shock protein 70, putative	237836239	−1.7	0.091	−2.0	0.042	1.1	0.64	0.027
84	Heat shock 70 kDa protein 8-like, PREDICTED:	291230940	−2.3	0.021	−2.3	0.053	1.1	0.59	0.0067
393	Nucleoredoxin	193890965	2.2	0.023	2.1	0.018	1.5	0.2	0.015
Carbon metabolism									
322	Ribulose 1,5-bisphosphate carboxylase oxygenase form II	37727264	−1.7	0.073	−2.0	0.057	−1.0	0.95	0.041
324	Ribulose 1,5-bisphosphate carboxylase oxygenase form II	37727264	−2.0	0.089	−2.2	0.071	1.1	0.78	0.047
666	PCP apoprotein precursor	75244617	−56.9	0.0013	−28.5	0.0024	−1.2	0.58	7.60E-05
507	PCP apoprotein precursor	23986649	−3.4	0.024	−2.4	0.09	−1.3	0.35	0.05
573	PCP apoprotein precursor	23986649	−3.6	0.0062	−3.0	0.0081	−1.3	0.33	0.0077
587	PCP apoprotein precursor	23986649	−3.6	0.022	−2.4	0.088	−1.2	0.42	0.048
1001	Light-harvesting polyprotein precursor	3355306	3.9	0.03	3.2	0.072	−1.2	0.83	0.02
376	Phosphoglycerate kinase	71033689	−1.7	0.093	−2.0	0.036	1.1	0.71	0.026
463	Pyruvate kinase	52550385	−3.2	0.025	−3.1	0.021	1.1	0.78	0.0026
492	Chloroplast glyceraldehyde-3-phosphate dehydrogenase	58618206	−3.0	0.011	−3.8	0.0092	1.1	0.79	0.0008
495	Glyceraldehyde-3-phosphate dehydrogenase	380235679	−2.4	0.052	−2.6	0.048	−1.1	0.82	0.035
497	Glyceraldehyde-3-phosphate dehydrogenase	380235679	−2.0	0.069	−2.3	0.056	−1.0	0.96	0.033
503	Chloroplast phosphoglycerate kinase	58613473	−2.1	0.049	−2.4	0.042	−1.1	0.72	0.027
530	Citrate lyase	83591557	−3.1	0.012	−3.8	0.0088	−1.1	0.84	0.0018
Protein and amino acid metabolism									
361	Translation elongation factor Tu	85703985	−2.0	0.076	−2.1	0.048	1.09	0.064	0.043
309	Adenosylhomocysteinase	211939908	−2.2	0.05	−2.0	0.013	1.2	0.43	0.058
291	Methionine S-adenosyltransferase	225685867	−2.6	0.055	−2.8	0.058	−1.1	0.86	0.031
294	Methionine adenosyltransferase	158524694	−3.0	0.027	−3.0	0.027	1.0	0.82	0.0014
759	L-3-phosphoserine phosphatase	255965821	−2.5	0.028	−1.9	0.07	−1.1	0.58	0.029
769	L-3-phosphoserine phosphatase	255965821	−1.9	0.033	−2.1	0.024	−1.2	0.42	0.029
775	L-3-phosphoserine phosphatase	255965821	−2.9	0.013	−2.2	0.03	−1.3	0.32	0.021
Lipid metabolism									
413	3-hydroxy-3-methylglutaryl-CoA lyase	81562665	−3.9	0.0015	−2.8	0.0089	−1.3	0.27	0.0075
Transport									
216	Iron compound ABC transporter, iron compound-binding protein	81714831	2.3	0.014	2.1	0.018	1.4	0.34	0.028
469	Mitochondrial import inner membrane translocase subunit tim50	74581880	2.0	0.008	2.1	0.014	1.5	0.11	0.028
188	ABC sugar (glycerol) transporter, periplasmic binding protein	149200989	2.9	0.034	2.8	0.023	1.1	0.82	0.0078
Hypothetical protein									
595	Hypothetical protein	145520727	−4.0	0.0089	−3.6	0.0068	−1.2	0.52	0.002
222	Hypothetical protein	145520727	4.0	0.011	3.8	0.011	1.8	0.41	0.017

[a]Spot ID represents the protein spot number on the two-dimensional fluorescence differential gel electrophoresis gels.
[b]Accession numbers according to the NCBI database.
[c]Spot abundance is expressed as the average ratio of intensities of up-regulated (negative values) or down-regulated (negative values) proteins at N-deplete, N-resupplied-2h and N-resupplied-26h compared with N-replete.
ABC, ATP-binding cassette; ANOVA, analysis of variance; PCP, peridinin chlorophyll *a* binding protein.

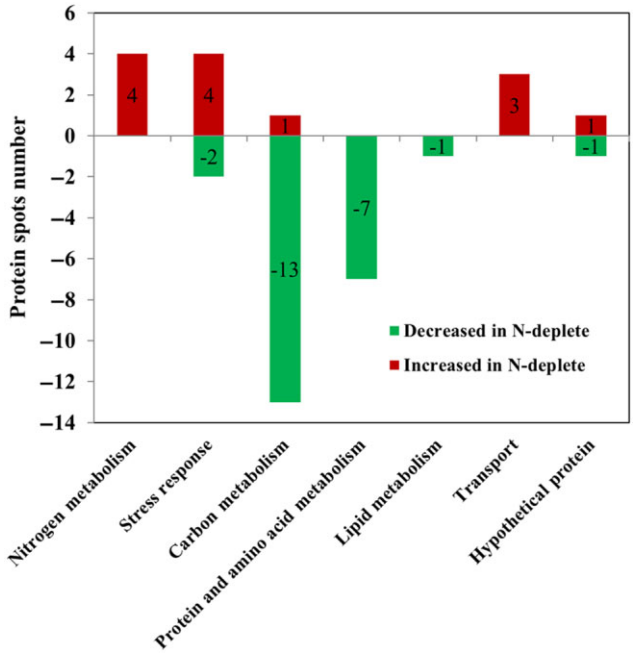

Figure 4. The biological processes of altered proteins associated with the nitrogen response of *Prorocentrum donghaiense*. Categorization is based on GO.

Unidentified protein spots are listed in Supporting Information Table S5.

The biological processes of the identified proteins were grouped based on the biological process of Gene Ontology (GO) classification (Fig. 4). Overall, proteins involved in carbon metabolism and stress response were up- or down-regulated in N-deplete cells, while proteins involved in N metabolism and transport were up-regulated, and proteins participating in protein and amino acid metabolism were down-regulated.

Proteins involved in carbon metabolism altered significantly in abundance in N-deplete cells. The abundance of one peridinin Chl *a* binding protein (PCP) apoprotein precursor isoform (spot 666) decreased by 56.9-fold in N-deplete cells, but it quickly recovered to its normal level after resupplying N. The other three PCP apoprotein precursor isoforms (spots 507, 573 and 587) were also down-regulated. Two isoforms of RuBisCo form II (spots 322 and 324) decreased 1.7 and twofold in abundance in N-deplete cells, and decreased two- and 2.2-fold in N-resupplied-2h cells, but they recovered to normal levels in N-resupplied-26h cells. Glyceraldehyde-3-phosphate dehydrogenase (GAPDH, spots 495 and 497), chloroplast GAPDH (spot 492), chloroplast phosphoglycerate kinase (spots 503), phosphoglycerate kinase (spots 376) and citrate lyase (spot 530) decreased by 1.7- to 3.1-fold in abundance in N-deplete cells and by two- to 3.8-fold in N-resupplied-2h cells, but they recovered to normal levels in N-resupplied-26h cells. The abundance of pyruvate kinase (spot 463) decreased 3.2- and 3.1-fold in N-deplete and N-resupplied-2h cells, but it recovered to the normal level in N-resupplied-26h cells. The 3-hydroxy-3-methylglutaryl- coenzyme A (CoA) lyase (spot 413) decreased 3.9- and 2.8-fold in the N-deplete and N-resupplied-2h cells, and then recovered to the normal level in N-resupplied-26h cells. However, the light-harvesting polyprotein precursor increased 3.9- and 3.2-fold in N-deplete and N-resupplied-2h cells, and then recovered to the normal level in N-resupplied-26h cells.

Four GS isoforms (spots 260, 263, 264 and 278) involved in N assimilation were identified and they were all significantly up-regulated in N-deplete and N-resupplied-2h cells. However, their abundances decreased remarkably in N-resupplied-26h cells. Three 60 kDa chaperonin (GroEL) isoforms (spots 207, 211 and 245) also presented high abundances in N-deplete and N-resupplied-2h cells (up to two- to 3.2-fold); however, two stress response proteins, heat shock protein 70 (HSP70, spot 80) and heat shock 70 kDa protein 8-like (spot 84) were down-regulated in N-deplete cells. Nucleoredoxin (NRX, spot 393) increased about twofold in the N-deplete and N-resupplied-2h cells, then decreased to the normal level in N-resupplied-26h cells. The translation elongation factor Tu (EF-Tu, spot 361) involved in protein synthesis decreased twofold in N-deplete and N-resupplied-2h cells, and recovered to the normal level in N-resupplied-26h cells. Three L-3-phosphoserine phosphatase isoforms (spots 759, 769 and 775) decreased by 1.9- to 2.9-fold in N-deplete and N-resupplied-2h cells, then recovered to normal levels in N-resupplied-26h cells. Adenosylhomocysteinase (spot 309), methionine adenosyltransferase (spot 294) and methionine S-adenosyltransferase (spot 291) decreased by 2.2- to 3-fold in abundance in the N-deplete and N-resupplied-2h cells, then recovered to normal levels in N-resupplied-26h cells. Three transport proteins, ATP-binding cassette (ABC) sugar (glycerol) transporter (periplasmic binding protein, spot 188), iron compound ABC transporter (iron compound-binding protein, spot 216), and mitochondrial import inner membrane translocase subunit tim50 (spot 469) exhibited high expressions in the N-deplete and N-resupplied-2h cells (two- to 2.9-fold), but they recovered to normal levels in N-resupplied-26h cells (1.5- to 1.1-fold). Moreover, one hypothetical protein (spot 222) presented high expression in the N-deplete and N-resupplied-2h cells, while the other hypothetical protein (spot 595) exhibited low expression in the N-deplete and N-resupplied-2h cells.

Expression of RuBisCo form II of *P. donghaiense* under various N conditions

Western blot analysis was then conducted to validate RuBisCo form II expression identified using the 2-D DIGE approach. The result indicated that the changes in protein levels were generally consistent with the variations in 2-D DIGE analysis (Fig. 5). The expression of RuBisCo form II was significantly depressed in the N-deplete and N-resupplied-2h cells; however, it recovered to the normal level after 26h of N-resupplement ($P < 0.05$).

DISCUSSION

In this study, we carried out a comparative proteomic analysis of *P. donghaiense* grown in N-replete, N-deplete and

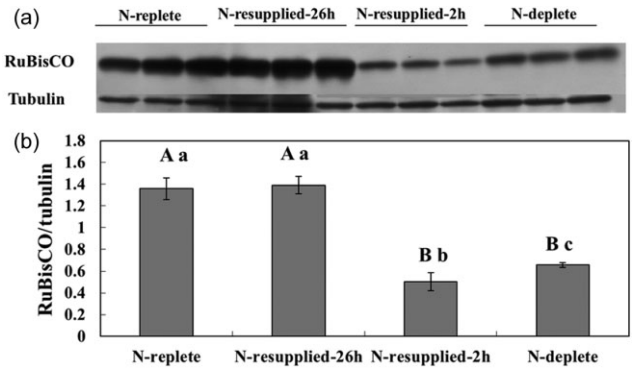

Figure 5. Western blot analysis of RuBisCo form II in *Prorocentrum donghaiense* cells under N-replete, N-resupplied-26h, N-resupplied-2h and N-deplete conditions. Intensities of the proteins were normalized to the corresponding tubulin level. (a) Representative Western blots. (b) Western blot results from densitometry analysis. Different capital letters and lowercase letters indicate statistically significant difference at $P < 0.01$ and $P < 0.05$, respectively.

N-resupplied conditions. A total of 37 out of the 56 altered protein spots were identified. Functional analyses of these N-responsive proteins revealed that proteins involved in photosynthesis, carbon fixation, and protein synthesis were down-regulated, whereas proteins participating in N reallocation and transport activity were up-regulated in N-deplete *P. donghaiense* cells. After resupplying N, most of the altered proteins recovered to normal levels within 26 h, indicating that *P. donghaiense* possessed a rapid response capability to changing N concentrations.

Carbon metabolism in N-deplete cells

In our study, N-depletion significantly depressed the expressions of most proteins involved in cellular carbon metabolism, that is photosynthesis, glycolysis, Calvin cycle and fatty acid biosynthesis (Fig. 6).

The down-regulation of photosynthesis in response to N starvation is reported in photosynthetic eukaryotes (Hockin *et al*. 2012; Dong *et al*. 2013). In our study, we found that the RuBisCo form II isoforms decreased about twofold in N-deplete and N-resupplied-2h cells, and the Western blot result also proved this. A similar result is also observed in N-deplete *A. affine* and *Alexandrium catenella* DH01 (Lee *et al*. 2009; Wang *et al*. 2012). RuBisCo, including forms I, II and III, catalyses the first step of the Calvin cycle of photosynthesis (Miziorko & Lorimer 1983), in which carbon is brought into the cellular metabolism in the form of CO_2, and also catalyses the oxidation of ribulose bisphosphate in the first step of photorespiration (Eisenberg *et al*. 1987). Dinoflagellates are the only group of eukaryotes known to harbour RuBisCo form II that has a much lower specificity for CO_2 over O_2 compared with the more common 'eukaryotic' RuBisCo found in other algae (Shi *et al*. 2013). It was also found that the abundance of the PCP apoprotein precursor isoforms decreased significantly to up to just under 60-fold change in N-deplete cells. PCP complexes, located peripherally on thylakoid membranes in close association with other components of the photosynthetic apparatus, function to absorb blue-green light and transduce it with high efficiency to the photochemical reaction centres (Prezelin 1987). The variability in PCP content determines dinoflagellate cell colour, and influences their light-harvesting capabilities and the optical properties of the water column (Prezelin & Boczar 1986). The down-regulations of RuBisCo form II and PCP apoprotein precursor in N-deplete *P. donghaiense* cells indicated that N-depletion depressed the photosynthetic capacity of *P. donghaiense*. The reduction of the photochemical efficiency of PSII (*Fv/Fm*) in N-deplete cells also supported this conclusion. Consistent with the decreased photosynthetic activity, proteins involved in the Calvin cycle and glycolysis such as pyruvate kinase, GAPDH and phosphoglycerate kinase were also down-regulated in N-deplete *P. donghaiense* cells. However, these results differed from a recent study of the diatom *Thalassiosira pseudonana* where glycolytic activity was enhanced at the onset of N starvation, and several enzymes involved in glycolysis were up-regulated (Hockin *et al*. 2012). This discrepancy might have been caused by species-specific differences and/or the duration of N starvation, but this needs further study in the future.

It is interesting that the light-harvesting polyprotein precursor (spot 1001) was remarkably up-regulated in N-deplete *P. donghaiense* cells. Light-harvesting complex (LHC) proteins function in photosynthesis by binding Chl and carotenoid molecules that absorb light and transfer the energy to the reaction centers of the photosystem, and a family of LHCs binding Chl *a* and *c* are found in dinoflagellates (Hiller *et al*. 1993, 1995; Boldt *et al*. 2012). Dinoflagellates can encode multiple nuclear-encoded plastid-targeted proteins translated as polyprotein precursors (Koziol & Durnford 2008). The principle light-harvesting Chl *a*-*c*-binding protein (19 kDa) of the dinoflagellate *Amphidinium carterae* is encoded as a polyprotein translated from a 6.1 kb mRNA (Hiller *et al*. 1995). Up-regulation of the light-harvesting polyprotein precursor in our study suggested that the N-deplete cells with low photosynthetic activity might not acquire many LHC proteins to harvest light compared with N-replete cells and, as a feedback, immature LHC proteins were accumulated in the cells as the light-harvesting polyprotein precursor. A recent study on the green alga *Nannochloropsis oceanica* IMET1 supports our suggestion in that LHC isoforms decreased by 1.5- to 2.5-fold in long-term N deprivation (Dong *et al*. 2013).

In some photosynthetic eukaryotes, photosynthesis still occurs when N is limiting and carbon skeletons can accumulate (Dagenais-Bellefeuille & Morse 2013). In higher plants and some algal species, intracellular excess carbon is stored in molecular pools during N limitation, with the form being starch in *Arabidopsis* (Peng *et al*. 2007a) and *Chlamydomonas reinhardtii* (Wase *et al*. 2014), and fatty acid and chrysolaminaran in *C. reinhardtii* (Blaby *et al*. 2013; Wase *et al*. 2014) and *N. oceanica* IMET1 (Dong *et al*. 2013). These carbon-accumulating processes increase specific gene

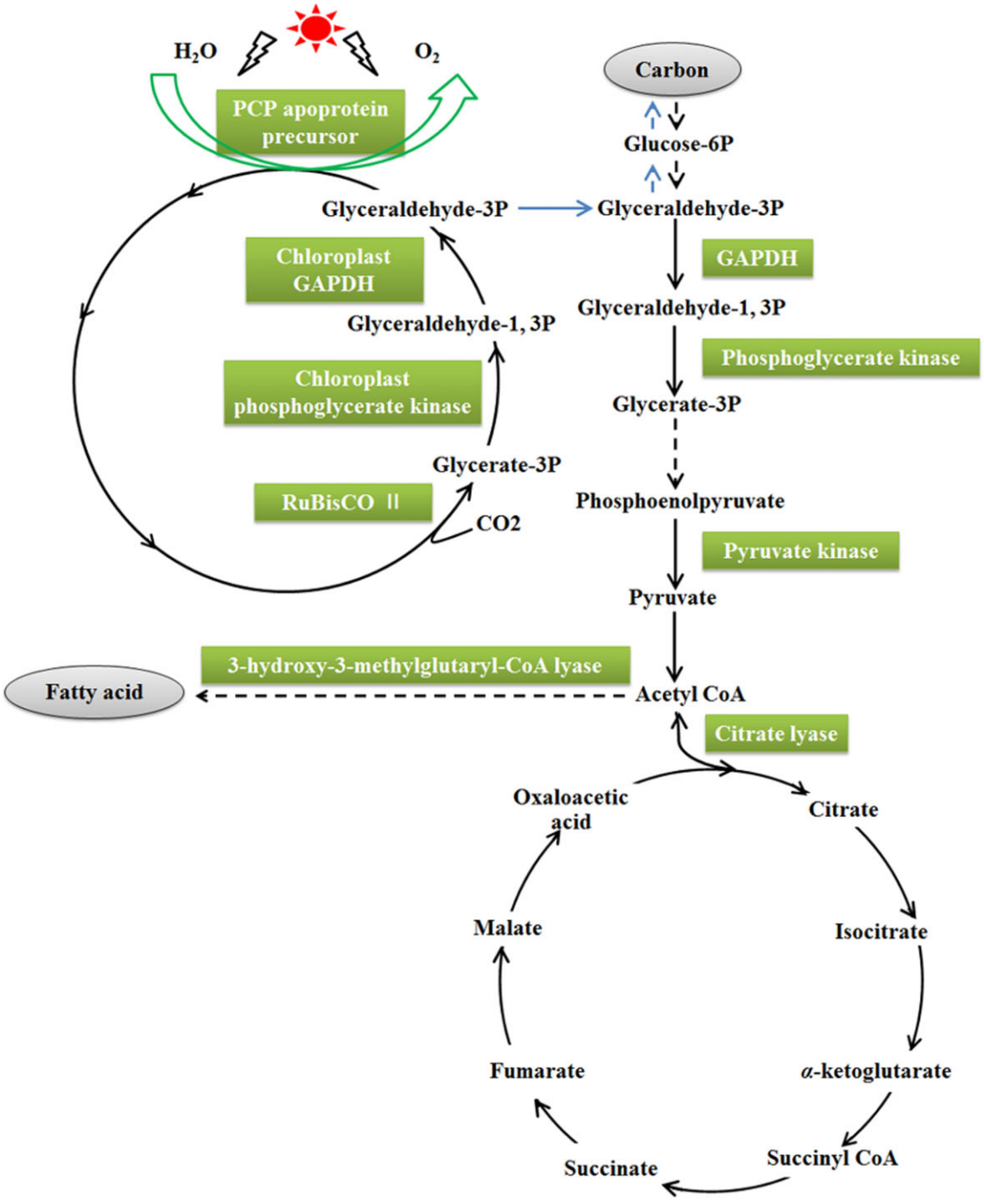

Figure 6. Proposed scheme for carbon metabolism in N-deplete cultures. The proteins in green boxes were down-regulated and no proteins were up-regulated. Solid arrows represent a one-step reaction while dashed arrows represent a multi-step reaction.

transcription and translation. In *Arabidopsis thaliana*, expressions of two genes involved in starch biosynthesis are increased at the transcription level under N limitation (Peng *et al*. 2007a). In *C. reinhardtii*, proteins involved in starch and lipid metabolism are elevated under nitrogen starvation culture (Wase *et al*. 2014). In long-term N-stressed *N. oceanica* IMET1, the proteins involved in fatty acid synthesis are up-regulated sharply and glycolysis is induced to make acetyl-CoA for fatty acid synthesis (Dong *et al*. 2013). Differing from the higher plants and green algae, *T. pseudonana* appears to remobilize intracellular carbon through increasing glycolytic proteins and their transcripts at the onset of N starvation (Hockin *et al*. 2012). In our study, no protein directly participating in starch or chrysolaminaran synthesis was identified although the POC content maintained a high level in N-deplete cells, and two key enzymes,

citrate lyase and 3-hydroxy-3-methylglutaryl-CoA lyase involved in fatty acid biosynthesis, were down-regulated in N-deplete cells, indicating that fatty acid biosynthesis was depressed by N-deficiency. These results suggested that *P. donghaiense* possessed a different mechanism for the regulation of intracellular carbon metabolism during N stress compared with other photosynthetic eukaryotes.

Protein and amino acid metabolism in N-deplete cells

Protein is considered to be the major macromolecular pool of intracellular N (Zhao *et al*. 2009; Lai *et al*. 2011) and N-deplete cells contain low protein content (Berdalet *et al*. 1994; Kilham *et al*. 1997; Lai *et al*. 2011). To maintain essential physiological functions for surviving in N-limited ambient conditions, cells usually degrade intracellular proteins to provide N sources (Thompson & Vierstra 2005; Peng *et al*. 2007a). The ubiquitin proteolytic pathway is a major system for selective protein degradation in eukaryotic cells. In the *Arabidopsis* N limitation adaptation (*nla*) mutant, the responsible gene *NLA* encodes a RING-type ubiquitin ligase that functions as a positive regulator controlling *Arabidopsis* adaptation to N limitation (Peng *et al*. 2007b). A recent study indicates that N-starvation enhances protein degradation in the diatom *T. pseudonana*: three proteases and a serine carboxypeptidase are found to increase in abundance in N-starved cells (Hockin *et al*. 2012). In our study, protein degradation-related proteins were not identified; however, cellular protein content in N-deplete cells was much lower than that in N-replete cells (Supporting Information Fig. S1), indicating the occurrence of protein degradation in N-deplete cells.

Reducing protein synthesis is another important way for cells to adapt to ambient N-limitation. In N starved *T. pseudonana*, two ribosomal proteins and a translation factor involved in protein biosynthesis are down-regulated (Hockin *et al*. 2012). In our study, we found that EF-Tu was down-regulated in N-deplete cells. EF-Tu is an abundant, highly conserved cellular guanosine triphosphate (GTP)-protein, occupying a key position in translation and plays an important role in protein biosynthesis (Sanderova *et al*. 2004). The down-regulation of EF-Tu in our study suggested that protein biosynthesis was inhibited in N-deplete *P. donghaiense* cells. This result was similar to the decrease of a translation elongation factor Ts during long-term N deprivation of *N. oceanica* IMET1 (Dong *et al*. 2013). HSP70 is one of the major classes of chaperone molecules and plays many roles in eukaryotic cells including protein synthesis and folding (Aparicio *et al*. 2005). In our study, HSP70 was down-regulated in N-deplete *P. donghaiense* cells, which might have been caused by low-protein biosynthesis. Consistent with this result, the abundances of adenosylhomocysteinase, L-3-phosphoserine phosphatase and methionine adenosyltransferase declined in N-deplete *P. donghaiense* cells. These proteins participate in the biosynthesis of amino acids, such as homocysteine, adenosine, methionine and serine. Down-regulation of these proteins indicated that amino acid synthesis was depressed in N-deplete cells, which subsequently affected the protein biosynthesis.

N metabolism in N-deplete cells

Nitrate reductase (NR), nitrite reductase (NiR), glutamate synthase (also known as glutamine oxoglutarate aminotransferase, GOGAT) and GS are essential N assimilating enzymes in photosynthetic algae: nitrate taken up into the cells is first reduced to nitrite by NR, then nitrite is further reduced to ammonium by NiR. Finally, ammonium is assimilated into amino acids and other nitrogenous compounds through GS and GOGAT (Glass *et al*. 2009). The coupled action of GS and GOGAT, often called the GS/GOGAT pathway, is thought to be the main pathway for the assimilation of ammonia in higher plants and algae (Anderson & Burris 1987). Expressions of GS and GOGAT are up-regulated in the N-deplete diatom *T. pseudonana* (Hockin *et al*. 2012), and the green alga *C. reinhardtii* (Wase *et al*. 2014) and *N. oceanica* IMET1 (Dong *et al*. 2013). The mRNA level of the GS gene is low in cells grown in the presence of ammonium, but a two- to fourfold increase is observed in cells grown in both nitrate-containing and N-deplete *C. reinhardtii* (Wase *et al*. 2014). The up-regulation of a cytosolic GS (GSIII) at the RNA level is also observed in the N-deplete dinoflagellate *Karenia brevis* (Morey *et al*. 2011). It is believed that dinoflagellates prefer to take up NH_4^+, which is principally assimilated through the GS/GOGAT pathway (Dagenais-Bellefeuille & Morse 2013). In our study, GS expression was significantly up-regulated, up to eightfold. However, GOGAT as well as other N assimilation enzymes, such as NR and NiR were not detected, which might have been caused by the long-term exposure of *P. donghaiense* cells to extreme ambient N deficiency. In many previous studies, algal cells were exposed to short-term N starvation or limitation, which might not cause serious N stress. However, in our study, N-deplete *P. donghaiense* cells were grown in the seawater with undetectable N for 7 d, N became an extreme stress to cells, which might depress the expressions of GOGAT as well as NR and NiR. It is reported that expression of GS varies with the growth time in N-stressed conditions. A study on the cyanobacterium *Synechococcus* strain PCC 7942 indicates that GS III (product of *glnN*) helps to cope with prolonged periods of N-starvation (extreme N-starvation) instead of short-term N-depletion (Sauer *et al*. 2000). A similar result is also found in N-stressed *C. reinhardtii* in which GS is up-regulated twofold in 24 h N-stressed cells to fourfold in 144 h N-stressed cells. However, GOGAT is up-regulated less than twofold through the whole experiment (Wase *et al*. 2014). Overall, these results suggest that GS play an important role in cell survival in N-deplete conditions.

In our study, the expression of GroEL presented a similar tendency for variation as did the GS, indicating that N-depletion led to GroEL folding GS in *P. donghaiense*. The folding and assembly of *Escherichia coli* dodecameric GS is facilitated by the GroEL (Tsuprun *et al*. 1992; Fisher 1998; Voziyan & Fisher 2000, 2002; Rajaram & Apte 2008).

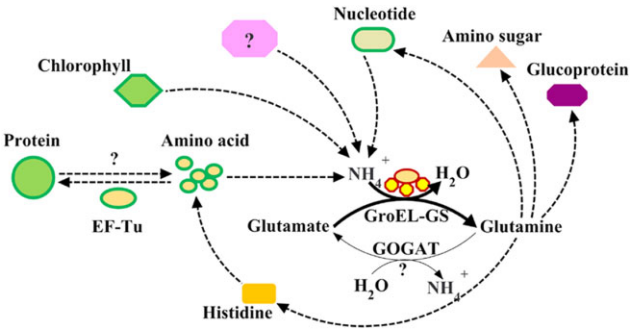

Figure 7. Proposed scheme illustrating cellular events related to N metabolism and reallocation in N-deplete *Prorocentrum donghaiense* cells. Glutamine synthetase (GS) and GroEL were up-regulated, while elongation factor Tu (EF-Tu) was down-regulated, no GOGAT was detected. Solid arrows represent a one-step reaction and dashed arrows represent a multi-step reaction. Anabolic structural components, such as proteins, become the target for degradation and N recycling, and a non-toxic N carrier, glutamine, was synthesized as a temporary N storage and a protective agent against ammonium toxicity.

Increasing expression of the GroEL during heat shock in *E. coli* (Sherman & Goldberg 1994) and N fixation processes in *Rhizobium meliloti* (Rusanganwa & Gupta 1993) are also observed. The high expression of GroEL and GS might be an adaptive strategy of *P. donghaiense* to extreme ambient N stress and one important reason resulting in its success in coastal waters.

Many dinoflagellate species including *Alexandrium minutum* (Maguer *et al*. 2007), *A. catenella* (Collos *et al*. 2004), *Symbiodinium* spp. (Kopp *et al*. 2013) and other dinoflagellates (Dortch *et al*. 1984), are able to store large amounts of inorganic and organic N forms, and *A. catenella* can accumulate enough N within 2 h to satisfy its growth requirements for more than 24 h and this usually finishes before it starts to divide and therefore exhibits a storage rather than a growth response to a nutrient pulse (Collos 1986; Collos *et al*. 2004). In N-sufficient cells, the proportion of N stored as ammonium is greater than that stored as nitrate, whereas in N-deficient cells, both N compounds are equally stored in *A. minutum* (Maguer *et al*. 2007). Similarly, *Symbiodinium* spp. can assimilate ammonium, nitrate and aspartic acid, resulting in rapid incorporation of N into uric acid crystals, and forming temporary N storage in response to fluctuating environmental dissolved N availability (Kopp *et al*. 2013). A similar result is also observed in *Prorocentrum triestinum*, which is postulated to contain a large amount of intracellular N pools and can be utilized for cell maintenance in N-limited condition (Chan *et al*. 2004). In our study, the PON content maintained a relatively stable level in the whole N-deplete process, however, the GS activity increased fourfold in N-starved cells, suggesting that intracellular N reallocation occurred actively, and glutamine might be synthesized and accumulated as a temporary N storage in N-deplete cells (Fig. 7). This is very different to *T. pseudonana*, which reassimilates N only from catabolic processes through the ornithine-urea cycle (Hockin *et al*. 2012). Glutamine, a non-essential branched chain amino acid, is the most important non-toxic nitrogen carrier in various organisms (Newsholme *et al*. 2003). It participates in a variety of metabolic processes as a conditionally essential amino acid and the significance of glutamine to metabolic homeostasis is well established during periods of stress. As a protective agent, glutamine also plays an important role in removing excess ammonia, which is toxic to cells. The increasing capacity of intracellular N reassimilation via the GroEL-GS complex in N-deplete *P. donghaiense* cells might be an adaptive response to extreme ambient N stress.

Other important biological processes in N-deplete cells

In N-deplete *P. donghaien*se cells, ABC sugar (glycerol) transporter (periplasmic binding protein), iron compound ABC transporter (iron compound-binding protein) and mitochondrial import inner membrane translocase subunit tim50 (Tim50) were found to be up-regulated. Transport of ions and organic molecules among cellular organelles is mediated by different types of transporters (Peng *et al*. 2007a). The ABC transporter superfamily is the largest transporter family in both prokaryotic and eukaryotic organisms, and it transports specific molecules across lipid membranes. These proteins translocate a wide variety of biomolecules including sugars, amino acids, metal ions, peptides, proteins, and a large number of hydrophobic compounds and metabolites across extra- and intracellular membranes (Dean *et al*. 2001). Tim50 is crucial for guiding the precursors of matrix proteins to their insertion site in the inner membrane (Geissler *et al*. 2002). Overall, our results suggested that N depletion enhanced transporter activity, which helped cells absorb various inorganic or organic nutrients for maintaining the essential physiology in the N-deplete condition.

In our study, NRX was up-regulated in N-deplete *P. donghaiense* cells, suggesting that N-deplete cells enhanced the response strategy of reactive oxygen species (ROS) elimination. As a redox-sensitive protein, NRX belongs to the thioredoxin protein family and is known to be involved in the regulation of a variety of ROS-mediated signalling pathways (Korswagen 2006). Up-regulation of NRX might have been caused by the accumulated ROS in N-deplete cells.

It should be pointed out that 19 protein spots were not identified successfully owing to a lack of information in the genomic and proteomic database of the dinoflagellates. Some of these proteins might be involved in various biological processes including N-deplete adaptation. With an increasing genomic database of the dinoflagellates and the application of new proteomic approaches (i.e. a shotgun proteomic approach), it is likely that we will gain more information about the molecular processes involved in N-depletion and recovery on a proteomic scale, and this will no doubt improve our understanding of the adaptive mechanism of dinoflagellates to changing ambient N.

CONCLUSIONS

This study, for the first time, applied a quantitative proteomic approach to compare the global protein profiles of *P. donghaiense* grown in N-replete, N-deplete and N-resupplied conditions, and identified differentially expressed proteins. When *P. donghaiense* cells could not uptake N from the ambient environment, the adaptive response machinery was initiated. Proteins involved in photosynthesis, carbon metabolism and protein biosynthesis were down-regulated, while proteins participating in intracellular N reallocation and transport activity were up-regulated in N-deplete cells. However, they recovered to normal status after resupplying N for 26 h, indicating the rapid proteomic response of *P. donghaiense* to ambient N changes. Intracellular N remobilization played important roles in the adaptation to ambient N stress (Fig. 7). In N-deplete cells, anabolic structure components, such as proteins, become the target for degradation and N recycling, while a non-toxic nitrogen carrier, glutamine, might be massively synthesized as a temporary N storage and a protective agent against ammonium toxicity. GroEL and GS played the central role in adapting ambient N stress. Our results indicated that *P. donghaiense* possessed a specific ability, in contrast with other photosynthetic eukaryotic algae, for the regulation of intracellular carbon and N metabolism in response to extreme ambient N deficiency. This might be an adaptive strategy of *P. donghaiense* to changing ambient N and one important reason resulting in its frequent and extensive blooms in coastal waters.

ACKNOWLEDGMENTS

This work was partially supported by research grants from the National Natural Science Foundation of China (Project No.41230961 and 41425021), the Ministry of Science and Technology of the People's Republic of China (Project No. 2010CB428703 and 2011CB111507). D.-Z. Wang was also supported by the 'Ten Thousand Talents Program' for leading talents in science and technological innovation. We thank Professor John Hodgkiss from The University of Hong Kong for his help with English. We also thank Professor Yong-Guan Zhu (Institute of Urban Environment) for his valuable comments.

REFERENCES

Anderson D., Kulis D., Sullivan J., Hall S. & Lee C. (1990) Dynamics and physiology of saxitoxin production by the dinoflagellates *Alexandrium* spp. *Marine Biology* **104,** 511–524.

Anderson S.L. & Burris J.E. (1987) Role of glutamine-synthetase in ammonia assimilation by symbiotic marine dinoflagellates (*Zooxanthellae*). *Marine Biology* **94,** 451–458.

Aparicio F., Thomas C.L., Lederer C., Niu Y., Wang D. & Maule A.J. (2005) Virus induction of heat shock protein 70 reflects a general response to protein accumulation in the plant cytosol. *Plant Physiology* **138,** 529–536.

Barcelo-Batllori S., Kalko S.G., Esteban Y., Moreno S., Carmona M.C. & Gomis R. (2008) Integration of DIGE and bioinformatics analyses reveals a role of the antiobesity agent tungstate in redox and energy homeostasis pathways in brown adipose tissue. *Molecular & Cellular Proteomics: MCP* **7,** 378–393.

Berdalet E., Latasa M. & Estrada M. (1994) Effects of nitrogen and phosphorus starvation on nucleic acid and protein content of *Heterocapsa* sp. *Journal of Plankton Research* **16,** 303–316.

Blaby I.K., Glaesener A.G., Mettler T., Fitz-Gibbon S.T., Gallaher S.D., Liu B., . . . Merchant S. (2013) Systems-level analysis of nitrogen starvation-induced modifications of carbon metabolism in a *Chlamydomonas reinhardtii* starchless mutant. *The Plant Cell* **25,** 4305–4323.

Boldt L., Yellowlees D. & Leggat W. (2012) Hyperdiversity of genes encoding integral light-harvesting proteins in the dinoflagellate *Symbiodinium* sp. *PLoS ONE* **7,** e47456.

Boyer G., Sullivan J., Andersen R., Harrison P. & Taylor F. (1987) Effects of nutrient limitation on toxin production and composition in the marine dinoflagellate *Protogonyaulax tamarensis*. *Marine Biology* **96,** 123–128.

Chan L.L., Hodgkiss I.J., Wan J.M., Lum J.H., Mak A.S., Sit W.H. & Lo S.C. (2004) Proteomic study of a model causative agent of harmful algal blooms, *Prorocentrum triestinum* II: the use of differentially expressed protein profiles under different growth phases and growth conditions for bloom prediction. *Proteomics* **4,** 3214–3226.

Chapman A.D. & Pfester L.A. (2008) The effects of temperature, irradiance, and nitrogen on the encystment and growth of the freshwater dinoflagellates *Peridinium cinctum* and *P. willei* in culture (*Dinophyceae*). *Journal of Phycology* **31,** 355–359.

Collos Y. (1986) Time-lag algal growth dynamics: biological constraints on primary production in aquatic environments. *Marine Ecology Progress Series* **33,** 193–206.

Collos Y., Gagne C., Laabir M., Vaquer A., Cecchi P. & Souchu P. (2004) Nitrogenous nutrition of *Alexandrium catenella* (*Dinophyceae*) in cultures and in Thau Lagoon, Southern France. *Journal of Phycology* **40,** 96–103.

Costas E. (1990) Genetic-variability in growth-rates of marine dinoflagellates. *Genetica* **82,** 99–102.

Dagenais-Bellefeuille S. & Morse D. (2013) Putting the N in dinoflagellates. *Frontier in Microbiology* **4,** doi: 10.3389/fmicb.2013.00369, 1–14.

Dean M., Hamon Y. & Chimini G. (2001) The human ATP-binding cassette (ABC) transporter superfamily. *Journal of Lipid Research* **42,** 1007–1017.

Dong H.P., Williams E., Wang D.Z., Xie Z.X., Hsia R.C., Jenck A., . . . Place A.R. (2013) Responses of *Nannochloropsis oceanica* IMET1 to long-term nitrogen starvation and recovery. *Plant Physiology* **162,** 1110–1126.

Dortch Q., Clayton J. Jr., Thoresen S. & Ahmed S. (1984) Species differences in accumulation of nitrogen pools in phytoplankton. *Marine Biology* **81,** 237–250.

Eisenberg D., Almassy R.J., Janson C.A., Chapman M.S., Suh S.W., Cascio D. & Smith W.W. (1987) Some evolutionary relationships of the primary biological catalysts glutamine synthetase and RuBisCO. *Cold Spring Harbor Symposia on Quantitative Biology* **52,** 483–490.

Fawcett S.E. & Ward B.B. (2011) Phytoplankton succession and nitrogen utilization during the development of an upwelling bloom. *Marine Ecology Progress Series* **428,** 13–31.

Fisher M.T. (1998) GroE chaperonin-assisted folding and assembly of dodecameric glutamine synthetase. *Biochemistry (Moscow, Russia)* **63,** 382–398.

Flynn K., Franco J., Fernandez P., Reguera B., Zapata M., Wood G. & Flynn K. (1994) Changes in toxin content, biomass and pigments of the dinoflagellate *Alexandrium minutum* during nitrogen refeeding and growth into nitrogen or phosphorus stress. *Marine Ecology Progress Series* **111,** 99–109.

Geider R.J., LaRoche J., Greene R.M. & Olaizola M. (1993) Response of the photosynthetic apparatus of *Phaeodactylum tricornutum* (*Bacillariophyceae*) to nitrate, phosphate, or iron starvation. *Journal of Phycology* **29,** 755–766.

Geider R.J., MacIntyre H.L., Graziano L.M. & McKay R.M.L. (1998) Responses of the photosynthetic apparatus of *Dunaliella tertiolecta* (*Chlorophyceae*) to nitrogen and phosphorus limitation. *Europen Journal Phycology* **33,** 315–332.

Geissler A., Chacinska A., Truscott K.N., Wiedemann N., Brandner K., Sickmann A., . . . Rehling P. (2002) The mitochondrial presequence translocase: an essential role of Tim50 in directing preproteins to the import channel. *Cell* **111,** 507–518.

Glass J.B., Wolfe-Simon F. & Anbar A.D. (2009) Coevolution of metal availability and nitrogen assimilation in cyanobacteria and algae. *Geobiology* **7,** 100–123.

Gruber N. (2004) The dynamics of the marine nitrogen cycle and its influence on atmospheric CO2 variations. The ocean carbon cycle and climate. *NATO Science Series* **40,** 97–148.

Hackett J.D., Anderson D.M., Erdner D.L. & Bhattacharya D. (2004) Dinoflagellates: a remarkable evolutionary experiment. *American Journal of Botany* **91,** 1523–1534.

Heisler J., Glibert P.M., Burkholder J.M., Anderson D.M., Cochlan W., Dennison W.C., . . . Suddleson M. (2008) Eutrophication and harmful algal blooms: a scientific consensus. *Harmful Algae* **8,** 3–13.

Herzig R. & Falkowski P.G. (1989) Nitrogen limitation in *Isochrysis galbana* (*Haptophyceae*). I. Photosynthetic energy conversion and growth efficiencies. *Journal of Phycology* **25,** 462–471.

Hiller R.G., Wrench P.M., Gooley A.P., Shoebridgem G. & Breton J. (1993) The major intrinsic light-harvesting protein of *Amphidinium*: characterization and relation to other light-harvesting proteins. *Photochemistry and Photobiology* **57,** 125–131.

Hiller R.G., Wrench P.M. & Sharples F.P. (1995) The light-harvesting chlorophyll *a*-*c*-binding protein of dinoflagellates – a putative polyprotein. *FEBS Letters* **363,** 175–178.

Hockin N.L., Mock T., Mulholland F., Kopriva S. & Malin G. (2012) The response of diatom central carbon metabolism to nitrogen starvation is different from that of green algae and higher plants. *Plant Physiology* **158,** 299–312.

Howarth R.W. (1988) Nutrient limitation of net primary production in marine ecosystems. *Annual Review of Ecology and Systematics* **19,** 89–110.

Keller M., Selvin R.C., Claus W. & Guillard R.R.L. (1987) Media for the culture of oceanic ultraphytoplankton. *Journal of Phycology* **23,** 633–638.

Kilham S., Kreeger D., Goulden C. & Lynn S. (1997) Effects of nutrient limitation on biochemical constituents of *Ankistrodesmus falcatus*. *Freshwater Biology* **38,** 591–596.

Knap A., Michaels A., Close A., Ducklow H. & Dickson A. (1996) Protocols for the joint global ocean flux study (JGOFS) core measurements. JGOFS, Reprint of the IOC Manuals and Guides No. 29, UNESCO 1994 19.

Kolber Z., Zehr J. & Falkowski P. (1988) Effects of growth irradiance and nitrogen limitation on hotosynthetic energy conversion in photosystem II. *Plant Physiology* **88,** 923–929.

Kopp C., Pernice M., Domart-Coulon I., Djediat C., Spangenberg J.E., Alexander D.T., . . . Meibom A. (2013) Highly dynamic cellular-level response of symbiotic coral to a sudden increase in environmental nitrogen. *Mbio* **4,** e00052–13.

Korswagen H.C. (2006) Regulation of the Wnt/beta-catenin pathway by redox signaling. *Developmental Cell* **10,** 687–688.

Koziol A.G. & Durnford D.G. (2008) Euglena light-harvesting complexes are encoded by multifarious polyprotein mRNAs that evolve in concert. *Molecular Biology and Evolution* **25,** 92–100.

Lai J., Yu Z., Song X., Cao X. & Han X. (2011) Responses of the growth and biochemical composition of *Prorocentrum donghaiense* to different nitrogen and phosphorus concentrations. *Journal of Experimental Marine Biology and Ecology* **405,** 6–17.

Latasa M. & Berdalet E. (1994) Effect of nitrogen or phosphorus starvation on pigment composition of cultured *Heterocapsa* sp. *Journal of Plankton Research* **16,** 83–94.

Lee F.W., Morse D. & Lo S.C. (2009) Identification of two plastid proteins in the dinoflagellate *Alexandrium affine* that are substantially down-regulated by nitrogen-depletion. *Journal of Proteome Research* **8,** 5080–5092.

Lei Q.Y. & Lü S.H. (2011) Molecular ecological responses of dinoflagellate, *Karenia mikimotoi* to environmental nitrate stress. *Marine Pollution Bulletin* **62,** 2692–2699.

Li J., Glibert P.M. & Alexander J.A. (2011b) Effects of ambient DIN : DIP ratio on the nitrogen uptake of harmful dinoflagellate *Prorocentrum minimum* and *Prorocentrum donghaiense* in turbidistat. *Chinese Journal of Oceanology and Limnology* **29,** 746–761.

Li T.S., Yu R.C. & Zhou M.J. (2011a) Short-term effects of different nitrogen substrates on growth and toxin production of dinoflagellate *Alexandrium catenella* Balech (strain ACDH). *Harmful Algae* **12,** 46–54.

Litchman E., Neale P.J. & Banaszak A.T. (2002) Increased sensitivity to ultraviolet radiation in nitrogen-limited dinoflagellates: photoprotection and repair. *Limnology and Oceanography* **47,** 86–94.

Lu J.Y. (2004) *The typical algal bloom species along the coastal waters of the China Sea – the study of the nutrient physiology of Proropcentrum donghainese Lu*. MS thesis, Xiamen University, Xiamen, China.

McGillicuddy D.J., Anderson D.M., Lynch D.R. & Townsend D.W. (2005) Mechanisms regulating large-scale seasonal fluctuations in *Alexandrium fundyense* populations in the Gulf of Maine: results from a physical-biological model. *Deep-Sea Research Part II, Topical Studies in Oceanography* **52,** 2698–2714.

McLachlan J.L., Marr J.C., Conlon-Kelly A. & Adamson A. (1994) Effects of nitrogen concentration and cold temperature on DSP-toxin concentrations in the dinoflagellate *Prorocentrum lima* (Prorocentrales, Dinophyceae). *Natural Toxins* **2,** 263–270.

Maguer J.F., Helguen L., Madec S., Labry C., Le C. & Corre P. (2007) Nitrogen uptake and assimilation kinetics in *Alexandrium minutum* (Dynophyceae): effect of N-limited growth rate on nitrate and ammonium interactions. *Journal of Phycology* **43,** 295–303.

Miziorko H.M. & Lorimer G.H. (1983) Ribulose-1, 5-bisphosphate carboxylase-oxygenase. *Annual Review of Biochemitry* **52,** 507–535.

Morey J.S., Monroe E.A., Kinney A.L., Beal M., Johnson J.G., Hitchcock G.L. & Van Dolah F.M. (2011) Transcriptomic response of the red tide dinoflagellate, *Karenia brevis*, to nitrogen and phosphorus depletion and addition. *BMC Genomics* **12,** 346.

Newsholme P., Lima M.M.R., Procopio J., Pithon-Curi T.C., Doi S.Q., Bazotte R.B. & Curi R. (2003) Glutamine and glutamate as vital metabolites. *Brazil Journal of Medical and Biological Research* **36,** 153–163.

Peng M., Bi Y.M., Zhu T. & Rothstein S.J. (2007a) Genome-wide analysis of *Arabidopsis* responsive transcriptome to nitrogen limitation and its regulation by the ubiquitin ligase gene *NLA*. *Plant Molecular Biology* **65,** 775–797.

Peng M., Hannam C., Gu H., Bi Y.M. & Rothstein S.J. (2007b) A mutation in *NLA*, which encodes a RING-type ubiquitin ligase, disrupts the adaptability of *Arabidopsis* to nitrogen limitation. *The Plant Journal* **50,** 320–337.

Prezelin B.B. (1987) Photosynthetic physiology of dinoflagellates. In *The Biology of Dinoflagellates* (ed. M. Taylor), pp. 174–223. Blackwell, London.

Prezelin B.B. & Boczar B.A. (1986) Molecular bases of cell absorption and fluorescence in phytoplankton: potential applications to studies in optical oceanography. In *Progress in Phycological Research* (eds F.E. Round & D.J. Chapman) Vol. **4,** pp. 349–364. Biopress, Bristol.

Rajaram H. & Apte S.K. (2008) Nitrogen status and heat-stress-dependent differential expression of the cpn60 chaperonin gene influences thermotolerance in the cyanobacterium *Anabaena*. *Microbiology (Reading, England)* **154,** 317–325.

Rusanganwa E. & Gupta R.S. (1993) Cloning and characterization of multiple groEL chaperonin-encoding genes in *Rhizobium meliloti*. *Gene* **126,** 67–75.

Sanderova H., Hulkova M., Malon P., Kepkova M. & Jonak J. (2004) Thermostability of multidomain proteins: elongation factors EF-Tu from *Escherichia coli* and *Bacillus stearothermophilus* and their chimeric forms. *Protein Science* **13,** 89–99.

Sauer J., Dirmeier U. & Forchhammer K. (2000) The *Synechococcus* strain PCC 7942 *glnN* product (glutamine synthetase III) helps recovery from prolonged nitrogen chlorosis. *Journal of Bacteriology* **182,** 5615–5619.

Sherman M. & Goldberg A.L. (1994) Heat shock-induced phosphorylation of GroEL alters its binding and dissociation from unfolded proteins. *Journal of Biological Chemistry* **269,** 31479–31483.

Shi X.G., Zhang H. & Lin S.J. (2013) Tandem repeats, high copy number and remarkable diel expression rhythm of form II RuBisCO in *Prorocentrum donghaiense* (Dinophyceae). *PLoS ONE* **8,** e71232.

Thompson A.R. & Vierstra R.D. (2005) Autophagic recycling: lessons from yeast help define the process in plants. *Current Opinion in Plant Biology* **8,** 165–173.

Tsuprun V.L., Boekema E.J., Pushkin A.V. & Tagunova I.V. (1992) Electron microscopy and image analysis of the GroEL-like protein and its complexes with glutamine synthetase from pea leaves. *Biochimica et Biophysica Acta* **1099,** 67–73.

Van Dolah F.V. (2000) Diversity of marine and freshwater algal toxins. In *Seafood and Freshwater Toxins: Pharmacology, Physiology, and Detection* (ed. L. Botana), pp. 19–44. CRC Press, Florida.

Voziyan P.A. & Fisher M.T. (2000) Chaperonin-assisted folding of glutamine synthetase under nonpermissive conditions: off-pathway aggregation propensity does not determine the co-chaperonin requirement. *Protein Science* **9,** 2405–2412.

Voziyan P.A. & Fisher M.T. (2002) Polyols induce ATP-independent folding of GroEL-bound bacterial glutamine synthetase. *Archives of Biochemistry and Biophysics* **397,** 293–297.

Wang D.Z. & Hsieh D.P.H. (2002) Effects of different nitrogen /phosphorus nutrient ratios on the growth and C2 toxin bioproduction in *Alexandrium tamarense* CI01. *Marine Pollution Bulletin* **45,** 286–289.

Wang D.Z., Li C., Xie Z.X., Dong H.P., Lin L. & Hong H.S. (2011) Homology-driven proteomics of dinoflagellates with unsequenced genomes using

MALDI-TOF/TOF and automated *de novo* sequencing. *Evidence-based Complementary and Alternative Medicine* **2011,** doi: 10.1155/2011/471020, 1–16.

Wang D.Z., Lin L., Wang M.H., Li C. & Hong H.S. (2012) Proteomic analysis of a toxic dinoflagellate *Alexandrium catenella* under different growth phases and conditions. *Chinese Science Bulletin* **57,** 3328–3341.

Wang D.Z., Zhang Y.J., Zhang S.F., Lin L. & Hong H.S. (2013) Quantitative proteomic analysis of cell cycle of the dinoflagellate *Prorocentrum donghaiense* (Dinophyceae). *PLoS ONE* **8,** e63659.

Wang M.H., Chan L.L., Si M.Z., Hong H.S. & Wang D.Z. (2010) Proteomic analysis of hepatic tissue of zebrafish (*Danio rerio*) experimentally exposed to chronic microcystin-LR. *Toxicological Science* **113,** 60–69.

Wang Y.J., Wang D.Z. & Hong H.S. (2009) Optimization of crude enzyme preparation methods for analysis of glutamine synthetase activity in phytoplankton and field samples. *Acta Oceanologica Sinica* **28,** 65–71.

Wase N., Black P.N., Stanley B.A. & DiRusso C.C. (2014) Integrated quantitative analysis of nitrogen stress response in *Chlamydomonas reinhardtii* using metabolite and protein profiling. *Journal of Proteome Research* **13,** 1373–1396.

Xu J., Ho A.Y.T., He L., Yin K.D., Hung C., Choi N., . . . Harrison P.J. (2012) Effects of inorganic and organic nitrogen and phosphorus on the growth and toxicity of two *Alexandrium* species from Hong Kong. *Harmful Algae* **16,** 89–97.

Zhang H. & Lin S.J. (2003) Complex gene structure of the form II Rubisco in the dinoflagellate *Prorocentrum minimum* (Dinophyceae). *Journal of Phycology* **39,** 1160–1171.

Zhao Y., Yu Z.M., Song X.X. & Cao X.H. (2009) Biochemical compositions of two dominant bloom-forming species isolated from the Yangtze River Estuary in response to different nutrient conditions. *Journal of Experimental Marine Biology and Ecology* **368,** 30–36.

Zhou M.J. (2010) Environmental settings and harmful algal blooms in the sea area adjacent to the Changjiang river estuary. *Coastal Environmental and Ecosystem Issue of the East China Sea* **2010,** 133–149.

Zhou M.J., Yan T. & Zou J.Z. (2003) Preliminary analysis of the characteristics of red tide areas in Changjiang estuary and its adjacent sea. *Chinese Journal of Applied Ecology* **14,** 1031–1038.

Received 28 July 2014; accepted for publication 5 March 2015

SUPPORTING INFORMATION

Additional Supporting Information may be found in the online version of this article at the publisher's web-site:

Figure S1. Cellular protein content of *Prorocentrum donghaiense* in N-replete, N-deplete, N-resupplied-2h and N-resupplied-26h conditions. Different capital letters and lowercase letters indicate statistically significant difference at $P < 0.01$ and $P < 0.05$, respectively.

Table S1. Proteins searched against NCBInr database.

Table S2. Peptides of proteins searched against NCBInr database.

Table S3. Proteins searched against dino-EST database.

Table S4. *De novo* sequencing and MS-BLAST.

Table S5. Unidentified proteins.